Testing Gravity with the Stacked Phase Space around Galaxy Clusters

Tsz Yan Lam,[1] Takahiro Nishimichi,[1] Fabian Schmidt,[2] and Masahiro Takada[1]

[1] *Kavli Institute for the Physics and Mathematics of the Universe (Kavli IPMU), University of Tokyo, Chiba 277-8583, Japan*
[2] *Theoretical Astrophysics, California Institute of Technology, Mail Code 350-17, Pasadena, California 91125*

In General Relativity, the average velocity field of dark matter around galaxy clusters is uniquely determined by the mass profile. The latter can be measured through weak lensing. We propose a new method of measuring the velocity field (phase space density) by stacking redshifts of surrounding galaxies from a spectroscopic sample. In combination with lensing, this yields a direct test of gravity on scales of 1-30 Mpc. Using N-body simulations, we show that this method can improve upon current constraints on $f(R)$ and DGP model parameters by several orders of magnitude when applied to upcoming imaging and redshift surveys.

PACS numbers: 98.80.Es, 04.50.+h, 04.80.Cc, 98.62.Sb
Keywords:

The accelerated expansion of the Universe is the most tantalizing problem in modern cosmology. Within Einstein's General Relativity (GR), the cosmic acceleration can be explained by introducing a mysterious smooth component, dark energy. However, it can also be interpreted as signature of the breakdown of GR on cosmological scales. Many on-going and upcoming wide-area galaxy surveys aim at testing dark energy and modified gravity scenarios as the origin of cosmic acceleration.

Cosmological probes of gravity are based on reconstructing the perturbations in the space-time metric and their relation to matter [1, 2]. Weak gravitational lensing provides a clean measurement of the lensing potential, while the timelike potential can be probed through the modulations in redshift caused by peculiar velocities of galaxies. In this *Letter*, we propose a new method of testing gravity at intermediate scales ($1 - 30$ Mpc) by measuring a projection of the position and velocity space (hereafter phasespace) around massive galaxy clusters. If GR is valid, the phasespace around the sampled clusters is uniquely determined by the mass density profile, which can be measured through stacked weak lensing. In other words, comparing the measured mass density and velocity profiles allows for a model-independent test of Einstein gravity. The scales probed are complementary to and potentially provide more information than the linear regime studied in most previous studies [3, 4], or the small scales considered in [5–8]. Moreover, this test is a *generic* probe of gravity: adding other, non-standard ingredients such as massive neutrinos or primordial non-Gaussianity, for example, will likely have a negligible impact on the relation between mass density and velocity profiles. This is not the case for other commonly considered probes of gravity, such as the matter power spectrum or cluster abundance. The main challenge lies in modeling the observables on these scales. We will demonstrate the feasibility of our method by using N-body simulations for Einstein and modified gravity models.

Methodology: Consider a sample of galaxy clusters (with accurate redshifts) in a cosmological volume covered by a spectroscopic galaxy survey. We can then construct the two-dimensional distribution of galaxy-cluster pairs in terms of the transverse distance r_p, and the relative line-of-sight velocity $v_{\rm los}$. More precisely, we have

$$r_p = d_A(z_c)\Delta\theta_{gc}, \quad v_{\rm los} = c(z_g - z_c), \tag{1}$$

where $\Delta\theta_{gc}$ is the angular separation of galaxy and cluster, d_A is the comoving angular diameter distance, c is the speed of light, and z_g, z_c denote the galaxy and cluster redshifts, respectively. The average phase space distribution is estimated by stacking all cluster-galaxy pairs.

The lower panel of Fig. 1 shows this distribution, using only peculiar motions, measured in the Einstein-gravity N-body simulations of [9] around halos with masses $M \geq 10^{14}\,M_\odot/h$ identified at $z = 0.35$, where we assumed a concordance Λ and cold dark matter cosmological model (ΛCDM). We use the output at $z = 0.35$ of 20 simulations of 1.5 $({\rm Gpc}/h)^3$ volume each. We defined halos using the friends-of-friends finder algorithm with linking length 0.2 times the mean particle separation, and assigned center-of-mass positions and velocities using the member particles. To mimic a galaxy redshift survey, we select secondary halos in the mass range $3 \times 10^{13} \leq M_s < 10^{14} M_\odot/h$ as galaxies in a cube of side length 40 Mpc$/h$ centered on each primary halo. In real galaxy surveys, such a selection in real space is not possible of course; we will return to this point below. By stacking over many clusters and binning in r_p, we average over triaxial or irregular density profiles, yielding a distribution which is only a function of r_p and $|v_{\rm los}|$.

The lower panel of Fig. 1 clearly shows two distinct regimes; at small radii $r_p \lesssim 2\,{\rm Mpc}/h$, iso-density contours are closed, while on larger scales the contours become open, reflecting the ongoing infall onto the massive halos. The boundary between these two regimes has been used in the caustic method [10]. As shown in a forthcoming paper, we can construct an accurate model of the $v_{\rm los} - r_p$ distribution of dark matter halos through a combination of N-body simulations and analytical theory. The upper panel shows the analytical prediction for the RMS dispersion of $v_{\rm los}$ as a function of r_p (estimated through the standard sample RMS). The model prediction is in good agreement with the simulation result, within the statistical errors of the simulation mea-

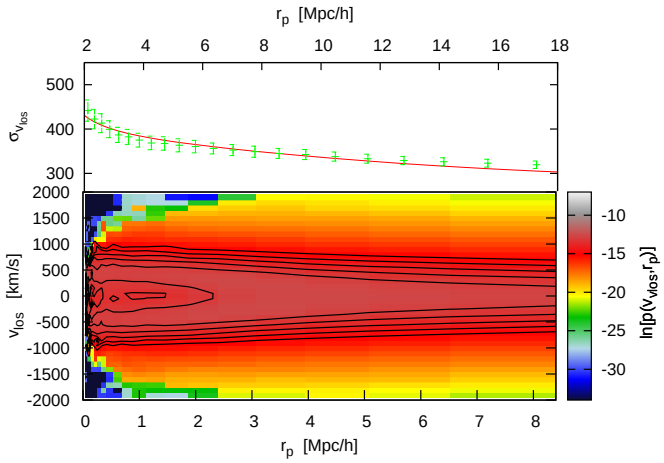

FIG. 1: *Lower panel*: The $v_{\rm los} - r_p$ phase space distribution (in logarithmic scale) as measured using halo catalogs constructed from N-body simulations in ΛCDM (see also [7]); we considered primary halos ("clusters") with masses $\geq 10^{14} M_\odot/h$ and secondary halos ("galaxies") in the range $3 \times 10^{13} \leq M \leq 10^{14}\ M_\odot/h$. *Upper panel*: The dispersion of the line-of-sight velocity distribution $\sigma_{v_{\rm los}}$ as function of r_p. The data points with error bars are computed from the simulation results in the lower panel, while the solid curve is our analytical model prediction. The error bars are scaled to mimic the measurement accuracies for a spectroscopic survey of 2000 sq. degrees over $0.2 < z < 0.4$.

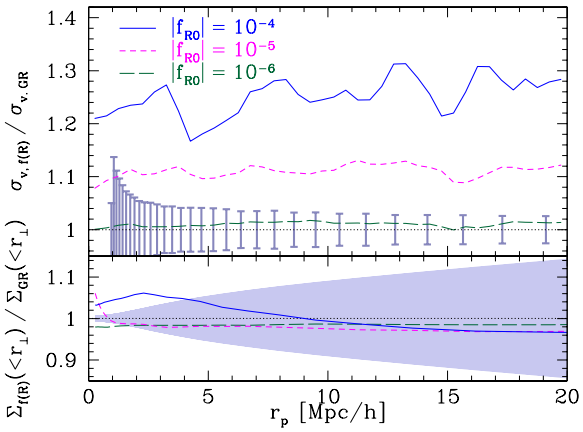

FIG. 2: *Upper panel:* Ratio of the velocity dispersion σ_v along the line of sight measured around halos with $M_{300} > 10^{14}\, M_\odot/h$ in $f(R)$ simulations to that measured around halos of the same mass in ΛCDM simulations. The error bars are estimated from the simulations, as in Fig. 1, for a spectroscopic survey of 2000 sq. degrees. *Lower panel:* Ratio of the enclosed projected mass profiles of the same halos in $f(R)$ and ΛCDM simulations. This is approximately what stacked lensing would measure. The shaed region indicates the range of statistical uncertainties for an imaging survey of the same area (see text).

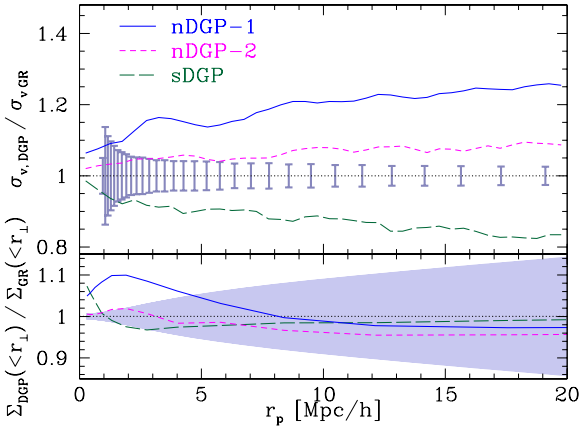

FIG. 3: Same as Fig. 2, but for DGP models (see text).

surements, which were measured from 20 simulation realizations so as to mimic the measurement accuracies for a survey of 2000 sq. degrees coverage and with redshift range $0.2 < z < 0.4$ (see below for more details). However, there are two complications that in reality need to be taken into account: the contribution to $v_{\rm los}$ from the cosmological redshift, which is given by $H\Delta r_{\rm los}$, where $\Delta r_{\rm los}$ is the line-of-sight separation between the galaxy and the cluster; and the contribution from motions of galaxies within their parent halos. The Hubble flow contribution can be modeled if the real-space cluster-galaxy correlation function on scales of interest is known. In practice, we can only measure the *redshift-space* correlation function, which in turn receives contributions from the velocities – this greatly complicates the subtraction of the Hubble flow contribution. One approach to solve this considerable difficulty is to construct a joint model of the $v_{\rm los} - r_p$ phase space and the redshift-space correlation function. Another possibility is to measure stacked weak lensing around the galaxies, which yields the real-space galaxy-matter correlation function. Combining the cluster-matter and galaxy-matter correlation can be used to infer the galaxy-cluster correlation function.

Another effect which has to be included is the motion of galaxies relative to the center-of-mass of their parent halos. In order to include this contribution, we need to know the distribution of relative velocities as well as radial offsets relative to their halos. If the galaxies are dynamically relaxed within the halos, these distributions are related by the virial theorem. Stacked weak lensing measured for the galaxy sample yields the mean parent halo mass as well as giving clues to the distribution of radial offsets. This can be used to constrain the galaxy motions within halos [11].

One further advantage of the stacking procedure and of considering scales of several Mpc is that we do not necessarily require a high number density of spectroscopic galaxies. In contrast, deep dedicated observations would be needed if one were to determine the velocity dispersion of individual clusters. The stacked weak lensing measurement requires an adequately deep imaging survey so that images of background galaxies are well resolved.

Results: We now turn to the signatures of modified

gravity in the $v_{\rm los} - r_p$ phase space. We begin with the modified action $f(R)$ model (see [12] and references therein), specifically the one of [13] with $n = 1$. The model can be parametrized by the amplitude f_{R0} of the scalar degree of freedom $f_R \equiv df/dR$ today, with $f_{R0} = 0$ being equivalent to ΛCDM. For the values considered here ($|f_{R0}| = 10^{-4} - 10^{-6}$), the expansion history is indistinguishable from ΛCDM. Current best cosmological constraints are a $|f_{R0}|$ <a few$\times 10^{-4}$ [14, 15]. In $f(R)$ gravity, gravitational forces are enhanced by a factor of 4/3 within the redshift-dependent Compton wavelength of the field. In addition, this model incorporates the chameleon mechanism which restores GR in high-density environments [13, 16]. The upper panel of Fig. 2 shows the dispersion σ_v of the line-of-sight velocity distribution in bins of r_p measured around halos above $10^{14}\,M_\odot/h$ in $f(R)$ N-body simulations [17, 18], relative to that measured in ΛCDM simulations around halos above the same mass threshold [27]. Due to the limited volume and resolution of the modified gravity simulations, we performed this measurement for dark matter particles. Note that the enhancements in σ_v can become significantly larger than the effect on the virial velocities, which are enhanced by up to a factor of $\sqrt{4/3} \approx 1.15$ in $f(R)$ [6].

In case of chameleon theories such as $f(R)$, if the spectroscopic galaxies are screened, we expect the enhancement of velocities to be suppressed [19]. Secondary halos with $M_{300} > 3 \times 10^{13}\,M_\odot/h$ identified in the $f(R)$ simulations indicate a somewhat suppressed effect on the velocity dispersion for $f_{R0} \leq 10^{-5}$, although the error bars are large. This suppression is consistent with the mass thresholds $\sim 10^{14}\,M_\odot/h$ and below for the chameleon mechanism for these field values [6]. On the other hand, the chameleon-screening of the clusters only affects the phase space at separations of order the virial radius of the cluster halos, i.e. a few Mpc or less. This can be seen for the cases of $f_{R0} = 10^{-5}, 10^{-6}$ in Fig. 2, for which the primary halos are screened in the simulations.

Fig. 3 shows the same measurement in N-body simulations of the Dvali-Gabadadze-Porrati (DGP) type braneworld models [20, 21]. We consider simulations for a self-accelerating DGP model without any Λ or dark energy (*sDGP*, [22]), and normal-branch models including a dark energy component (*nDGP*, [23]). The dark energy equation of state is adjusted to yield a ΛCDM expansion history, making these nDGP models indistinguishable by geometric probes [23]. In case of sDGP, we compare to a GR model with an effective dark energy yielding the same expansion history, in order to isolate the modified structure growth effects. DGP models are characterized by the cross-over scale r_c, above which gravity transitions from 4D to 5D. On scales below r_c, gravity is described by a 4D scalar-tensor theory, where the strength of the modified force scales with Hr_c. In sDGP, $r_c = 1.35 H_0^{-1} = 4038\,{\rm Mpc}/h = 6118$ Mpc, while in nDGP–1 (–2) it is taken to be 500 (3000) Mpc. As expected, we see that sDGP yields smaller velocities than GR, since gravity is weakened in the self-accelerating branch. Conversely, normal-branch models yield higher velocities. We find no indication of a suppression of the effect when considering secondary halos ($M_s > 3 \times 10^{13}\,M_\odot/h$) instead of dark matter, consistent with the fact that the Vainshtein screening mechanism inherent in these braneworld scenarios does not directly lead to a velocity bias [19].

Will upcoming surveys be able to detect such modified gravity signatures in the phase space distribution? The statistical uncertainties in σ_v arise from an imperfect sampling due to a finite number of the cluster-galaxy pairs and from cosmic variance due to a finite volume coverage. To make realistic forecasts, we adopt survey parameters that resemble the planned imaging and spectroscopic surveys with the Subaru Telescope [11]; we assume a survey area of 2000 square degrees, and consider as cluster sample halos with mass greater than $10^{14} M_\odot/h$ and in the redshift range $0.2 < z < 0.4$. The comoving volume corresponds to 0.23 $({\rm Gpc}/h)^3$. We chose the mass range so that the massive halos allow an accurate measurement of the average mass profile with weak lensing [24]. We choose a cluster sample at relatively low redshifts to allow for a denser sampling of redshifts of the secondary halos (galaxies). For the latter, we assume that the galaxies reside in halos with masses $3 \times 10^{13} \leq M_s < 10^{14} M_\odot/h$ as in Fig. 1, and assume one galaxy per halo residing at the halo's center of mass. The mean number densities of the primary and secondary halos, found from the ΛCDM simulations, are 1.7×10^{-5} and 8.3×10^{-5} $[{\rm Mpc}/h]^{-3}$, respectively, the latter being lower than the density of spectroscopic galaxies for the SDSS BOSS survey [25] or the target density for the Subaru survey.

To estimate the measurement accuracies, we divide each of our 20 realizations of N-body simulations for ΛCDM into 27 subvolumes of 0.056 $({\rm Gpc}/h)^3$ at the output redshift $z = 0.35$, in order to increase the sample size. We compute the stacked phase space distribution $(v_{\rm los}, r_p)$ and RMS $\sigma_v(r_p)$ using pairs in each subvolume. We then compute the mean and covariance of the σ_v-profiles for all radial bins over the 540 samples. Finally, we rescale the covariance by $(V_{\rm sim}/V_{\rm survey})^{1/2}$. The 1σ uncertainty in each radial bin is shown in the upper panel of Fig. 2 and 3. The constraining power of the assumed galaxy survey is clearly very significant, over a wide range of separations. Note that the error bars at different radial bins are highly correlated. To be more quantitative, we can estimate the value of $-2\Delta \ln \mathcal{L}$ between the ΛCDM and $f(R)$ models, using the full covariance of $\sigma_v(r_p)$ as measured in the ΛCDM simulations. This yields 218, 70 and 2.2 for $|f_{R0}| = 10^{-4}, 10^{-5}$ and 10^{-6}, respectively, assuming that the shape of the velocity profile is perfectly known. This shows that there is enough signal-to-noise to probe $f(R)$ gravity down to field values at which the secondary halos become chameleon-screened and this measurement loses its power. Adding a log-normal scatter in mass of $\sigma(\ln(M)) = 0.2$ in both primary and secondary halos changes the velocity profile by less than 5%. Hence the velocity profile appears to be robust with respect to

uncertainties in mass estimates of the halos.

For comparison, the lower panels of Fig. 2 and 3 show the ratio of the enclosed projected mass profiles around the primary halos in modified gravity to that in ΛCDM. This quantity can be reconstructed from weak lensing measurements, and has been used to constrain $f(R)$ gravity [26]. Clearly, the departures in the mass profile are much smaller than those in the velocities. The range enclosed by the two thin-solid curves shows the expected 1σ measurement uncertainties for a Subaru-type imaging survey covering the same region of the sky, i.e. 2000 square degrees. The lensing errors are determined by the survey area and the shot noise [24]; we assumed a background galaxy density at $z_s > 0.6$ of $\bar{n}_g = 22$ arcmin^{-2} and a RMS intrinsic ellipticity of $\sigma_\epsilon = 0.22$. Given the size of the error bars relative to the modified gravity effects, it is clear the lensing signal itself is a much less powerful probe of gravity than velocities.

Discussion: In this *Letter*, we have investigated a method of using the phase space distribution around massive clusters to constrain modified gravity models. Using collisionless numerical simulations for ΛCDM, $f(R)$ and DGP models, we demonstrated that the velocity dispersion as a function of transverse separation shows up to order unity deviations when compared to the profile in GR. On the other hand, the effect on the interior mass profile, which is measurable through stacked weak lensing, is much less affected by modifications to gravity. While we have concentrated on the second moment of the velocity distribution here, in principle even more information is contained in the higher moments. As working examples, we showed that a spectroscopic survey covering an area of 2000 square degrees can in principle yield greatly improved constraints on $f(R)$ and DGP models (see Figs. 2 and 3). The scales probed by this method are in the (weakly) nonlinear regime, and bridge the gap between the scales probed by redshift-space distortions in galaxy two-point correlations on large scales and virial velocities within halos on small scales. By combining these different methods, we can probe gravity properties over a wide range of scales, and have a better chance of capturing the signatures of the screening mechanisms, should the accelerated expansion in fact be due to the breakdown of Einstein gravity on cosmological scales.

TYL, TN and MT are supported in part by Grant-in-Aid for Young Scientists (Nos. 22740149 and 23340061) and by WPI Initiative, MEXT, Japan. Numerical calculations for the present work have been in part carried out under the Interdisciplinary Computational Science Program in Center for Computational Sciences, University of Tsukuba, and on Cray XT4 at Center for Computational Astrophysics, CfCA, of National Astronomical Observatory of Japan. FS is supported by the Gordon and Betty Moore Foundation at Caltech. MT is also supported by the FIRST program "Subaru Measurements of Images and Redshifts (SuMIRe)", CSTP, Japan.

[1] E. Bertschinger, Astrophys. J. **648**, 797 (2006), arXiv:astro-ph/0604485.
[2] B. Jain and P. Zhang, ArXiv e-prints **709** (2007), 0709.2375.
[3] P. Zhang, M. Liguori, R. Bean, and S. Dodelson, Physical Review Letters **99**, 141302 (2007), 0704.1932.
[4] R. Reyes, R. Mandelbaum, U. Seljak, T. Baldauf, J. E. Gunn, L. Lombriser, and R. E. Smith, Nature (London) **464**, 256 (2010), 1003.2185.
[5] J. Schwab, A. S. Bolton, and S. A. Rappaport, Astrophys. J. **708**, 750 (2010), 0907.4992.
[6] F. Schmidt, Phys. Rev. D **81**, 103002 (2010), 1003.0409.
[7] R. Wojtak, S. H. Hansen, and J. Hjorth, Nature (London) **477**, 567 (2011), 1109.6571.
[8] A. Boyarsky and O. Ruchayskiy, Physics Letters B **695**, 365 (2011), 2011PhLB..695..365B, 1001.0565.
[9] T. Nishimichi and A. Taruya, Phys. Rev. D **84**, 043526 (2011), 1106.4562.
[10] A. Diaferio and M. J. Geller, Astrophys. J. **481**, 633 (1997), arXiv:astro-ph/9911277.
[11] C. Hikage, M. Takada, and D. N. Spergel, MNRAS **419**, 3457 (2012), 1106.1640.
[12] T. P. Sotiriou and V. Faraoni (2008), 0805.1726.
[13] W. Hu and I. Sawicki, Phys. Rev. D **76**, 064004 (2007), arXiv:0705.1158.
[14] F. Schmidt, A. Vikhlinin, and W. Hu, ArXiv e-prints (2009), 0908.2457.
[15] L. Lombriser, A. Slosar, U. Seljak, and W. Hu, ArXiv e-prints (2010), 1003.3009.
[16] J. Khoury and A. Weltman, Phys. Rev. D **69**, 044026 (2004), arXiv:astro-ph/0309411.
[17] H. Oyaizu, Phys. Rev. D **78**, 123523 (2008), 0807.2449.
[18] F. Schmidt, M. Lima, H. Oyaizu, and W. Hu, Phys. Rev. D **79**, 083518 (2009), 0812.0545.
[19] L. Hui, A. Nicolis, and C. W. Stubbs, Phys. Rev. D **80**, 104002 (2009), 0905.2966.
[20] G. Dvali, G. Gabadadze, and M. Porrati, Physics Letters B **485**, 208 (2000), arXiv:hep-th/0005016.
[21] C. Deffayet, Physics Letters B **502**, 199 (2001), arXiv:hep-th/0010186.
[22] F. Schmidt, Phys. Rev. D **80**, 043001 (2009), 0905.0858.
[23] F. Schmidt, ArXiv e-prints (2009), 0910.0235.
[24] M. Oguri and M. Takada, Phys. Rev. D **83**, 023008 (2011), 1010.0744.
[25] M. White, M. Blanton, A. Bolton, D. Schlegel, J. Tinker, A. Berlind, L. da Costa, E. Kazin, Y.-T. Lin, M. Maia, et al., Astrophys. J. **728**, 126 (2011), 1010.4915.
[26] L. Lombriser, F. Schmidt, T. Baldauf, R. Mandelbaum, U. Seljak, and R. E. Smith, ArXiv e-prints (2011), 1111.2020.
[27] Although this measurement was done at $z = 0$, a comparison with the results at $z = 1$ shows that the enhancement in σ_v is only weakly redshift-dependent.